



HAL
open science

Toward a unified formulation of the acoustic transfer admittance of cylindrical cavities for reciprocity calibration of microphones

D Rodrigues, P Vincent

► **To cite this version:**

D Rodrigues, P Vincent. Toward a unified formulation of the acoustic transfer admittance of cylindrical cavities for reciprocity calibration of microphones. *Metrologia*, 2023, 60 (4), pp.1-16. 10.1088/1681-7575/ace3c4 . hal-04187421

HAL Id: hal-04187421

<https://cnam.hal.science/hal-04187421>

Submitted on 24 Aug 2023

HAL is a multi-disciplinary open access archive for the deposit and dissemination of scientific research documents, whether they are published or not. The documents may come from teaching and research institutions in France or abroad, or from public or private research centers.

L'archive ouverte pluridisciplinaire **HAL**, est destinée au dépôt et à la diffusion de documents scientifiques de niveau recherche, publiés ou non, émanant des établissements d'enseignement et de recherche français ou étrangers, des laboratoires publics ou privés.



Distributed under a Creative Commons Attribution 4.0 International License



PAPER • OPEN ACCESS

Toward a unified formulation of the acoustic transfer admittance of cylindrical cavities for reciprocity calibration of microphones

To cite this article: D Rodrigues and P Vincent 2023 *Metrologia* **60** 045012

View the [article online](#) for updates and enhancements.

You may also like

- [Frequency increase in resonant-tunneling diode cavity-type terahertz oscillator by simulation-based structure optimization](#)
Mikhail Bezhko, Safumi Suzuki and Masahiro Asada
- [Electrical admittance of a circular piezoelectric transducer and chargeless deformation effect](#)
Mojtaba Khayatizad, Mia Loccufier and Wim De Waele
- [FIRST QUINTUPLET FREQUENCY SOLUTION OF A BLAZHKO VARIABLE: LIGHT CURVE ANALYSIS OF RV UMa](#)
Zs. Hurta, J. Jurcsik, B. Szeidl et al.

Toward a unified formulation of the acoustic transfer admittance of cylindrical cavities for reciprocity calibration of microphones

D Rodrigues^{1,*}  and P Vincent²

¹ Laboratoire Commun de Métrologie LNE-CNAM (LCM), 29 Avenue Roger Hennequin, 78197 Trappes Cedex, France

² Commissariat à l'Énergie Atomique et aux énergies alternatives (CEA), DAM, DIF, F-91297 Arpajon Cedex, France

E-mail: dominique.rodrigues@lne.fr

Received 7 April 2023, revised 28 June 2023

Accepted for publication 4 July 2023

Published 18 July 2023



CrossMark

Abstract

The pressure reciprocity technique for calibration of Laboratory Standard microphones provides the basis for primary measurement standards for sound pressure. This calibration method is described in the International Electrotechnical Commission (IEC) standard 61094-2:2009 where the key aspect relating to the calculation of the acoustic transfer admittance of couplers was recently completed and clarified in the amendment IEC 61094-2:2009/AMD1:2022. Three models are currently provided for calculating this quantity: the low-frequency solution suitable to low frequencies, the extended low-frequency solution suitable to low and medium frequencies, and the broadband solution suitable to medium and high frequencies. It is established that neither of these models is correct for all frequencies routinely considered in many National Metrology Institutes, namely from 2 Hz to 25 kHz, so that a transition must be made. Based on the fundamental equations of acoustics in thermoviscous fluid, this paper provides a unified formulation for the acoustic transfer admittance of cylindrical cavities. Under the common quasi-plane wave approximation, this paper provides a new form of solution for the Fourier equation, not restricted by any assumption on the pressure variation and leading to a new form of propagation equation in the coupler. Two techniques are used to solve the problem, the Laplace Adomian Decomposition Method and a stepped duct approximation technique. Numerical results are presented, providing substantial evidence to support the validity of these formulations. A high level of agreement is observed between the two models, approximately 10^{-6} dB for the amplitude and 10^{-4} degrees for the phase, excluding the resonance frequencies of couplers. Finally, this paper evaluates the compatibility of the extended low-frequency solution provided in the IEC amendment with the fundamental equations established in this study. A new simplified solution is provided, highlighting discrepancies in the application of the heat conduction corrective factor as compared to the guidelines outlined in the IEC amendment.

* Author to whom any correspondence should be addressed.



Original Content from this work may be used under the terms of the [Creative Commons Attribution 4.0 licence](https://creativecommons.org/licenses/by/4.0/). Any further distribution of this work must maintain attribution to the author(s) and the title of the work, journal citation and DOI.

Supplementary material for this article is available [online](#)

Keywords: calibration, reciprocity, microphones, impedance, admittance, acoustics

(Some figures may appear in colour only in the online journal)

1. Introduction

The pressure reciprocity calibration method as specified in the International Electrotechnical Commission (IEC) Standard 61 094-2:2009 [1] is currently used worldwide for absolute pressure calibration of laboratory standard (LS) microphones, and provides the basis for primary measurement standards for sound pressure. This method, which is based on the use of closed couplers, is routinely applied by the national metrology institutes (NMIs) at frequencies from 2 Hz up to 25 kHz [2]. In the most usual configuration, the pressure reciprocity method requires three reciprocal microphones coupled by pairs using a cavity, generally with a cylindrical shape. The coupler ends are closed by the microphone diaphragms, with one being used as a transmitter and the other one as a receiver. The product of the microphone sensitivities is determined from electrical measurements and from analytical calculation of the acoustic transfer admittance of the system. Finally, this operation is repeated with the remaining paired combinations of microphones.

Calculation of the acoustic transfer admittance is a key aspect of microphone pressure reciprocity calibration. The acoustic transfer admittance, defined as the ratio of the short-circuit volume velocity produced by the transmitter microphone to the sound pressure acting on the diaphragm of the receiver microphone has been extensively explored and discussed considering both influence of heat conduction and viscous losses [3–14]. The IEC Standard 61 094-2:2009 [1] provides two formulations for calculation of the acoustic transfer admittance: (i) the *broadband solution*, which considers both thermal and viscous effects in plane wave couplers and is applicable to medium and high frequencies (plane-wave couplers have cavity diameters equal to the diameters of the microphone front cavities [1]), and (ii) the *low-frequency solution* where the influence of the heat conduction losses is expressed in terms of a complex correction factor Δ_H to the geometrical volume V of the coupler. Driven by the demand for traceable calibrations at infrasonic frequencies [15, 16], significant efforts were carried out recently to improve and extend the validity of the *low-frequency solution* to frequencies below 2 Hz, leading to the publication in 2022 of an amendment of the IEC standard 61 094-2:2009/AMD1:2022 [17]. Specifically, this amendment replaces the existing *low-frequency solution* with a new one, and also introduces a new model referred to hereafter as the *extended low-frequency solution*. This amendment was motivated by recent publications: (i) Vincent *et al*'s work in [13], which provides a clarified and improved analytical formulation of the correction factor Δ_H , and (ii) Sandermann

Olsen's work in [14], which presents a method for expanding the applicability of the solution proposed by Vincent *et al* to medium frequencies. The approach of calculation for this extended solution involves calculating the transfer admittance through the transmission line model, i.e. equation (4) of IEC 61 094-2:2009 where the correction factor Δ_H is applied to the cross sectional area, S in the characteristic acoustic admittance of plane wave coupler $Y_{a,0} = S/(\rho_0 c_0)$ (where ρ_0 is the density of the gas enclosed and c_0 the adiabatic speed of sound) and where the propagation constant is fixed to $k = 0 + j\omega/c_0$ (where ω is the angular frequency). The validity of this solution is mainly supported by its convergence with a solution provided by a finite element software. However, it would be beneficial to reinforce its reliability by developing an analytical model that establishes the limitations of the solution.

In summary, the IEC Standard 61 094-2:2009 and its recent amendment IEC 61 094-2:2009/AMD1:2022 provide three models for calculating the acoustic transfer admittance of cylindrical cavities, (i) the *low-frequency solution* (outlined in [17]) which is assumed to be valid at low frequencies where $\lambda > 100\sqrt{V}$ (with λ representing the wavelength) corresponding to frequencies below [300 Hz–700 Hz] for plane-wave couplers commonly used for reciprocity calibrations, (ii) the *extended low-frequency solution* (outlined in [17]) which is assumed to be valid at low and medium frequencies where $\lambda > 25\ell$ (where ℓ is the length of the cavity) corresponding to frequencies below [1000 Hz–3450 Hz] for the same plane-wave couplers, and (iii) the *broadband solution* (outlined in [1]) which is assumed to be valid at high frequencies where $\lambda < 16\ell a$ (where a is the radius of the cavity and the factor 16 being an empirical factor, expressed in m^{-1}) corresponding to frequencies above [175 Hz–1150 Hz] for the same plane-wave couplers.

The pressure reciprocity calibration of LS microphones in the frequency range 2 Hz–25 kHz is the norm now in many NMIs. Therefore, it can be established that neither of the standardized models is correct at all frequencies of interest. In fact, there is only just a frequency range where low and high frequency solutions can be considered reasonably accurate so that a transition must be made. In the [14], the author recommend as a compromise for calibrations to make a gradual transition between the solutions in a range of frequencies where both solutions are assumed to be valid. Although using this approach may be appropriate, it would be beneficial to use a valid unified formulation of the acoustic transfer admittance. Therefore, it is the aim of this paper to propose such unified formulation of the acoustic transfer admittance of cylindrical cavities relevant for reciprocity calibration of LS

microphones in the widest frequency range, and not restricted by any assumption about the relative size of the wavelength and coupler dimensions.

After establishing the fundamental equations of the problem, the paper presents two techniques for solving it: the Laplace Adomian decomposition method (LADM) and a stepped duct approximation technique. The resulting expressions for the acoustic transfer admittance for cylindrical cavities (commonly referred to as plane wave couplers) are given and calculated for several couplers commonly used for reciprocity calibrations. The results obtained are compared to those given in the IEC standard. Finally, this paper evaluates the compatibility of the *extended low-frequency solution* provided in the IEC amendment with the fundamental equations established in this study. It is important to mention that, while the paper includes results and discussions related to high frequencies, where the influence of radial wave motion cannot be disregarded in comparison to calibration uncertainties [18], the current formulation does not specifically address this issue. The conclusion further reflects on this crucial matter.

2. The equation of propagation for the quasi plane wave approximation

The considered domain Ω is a cylindrical cavity (length ℓ , radius a) closed at one end $z=0$ by the diaphragm of a transmitter microphone driven by a velocity v_t and at the other end $z=\ell$ by the diaphragm of a receiver microphone (figure 1).

The variables describing the dynamic and thermodynamic states of the fluid are the particle velocity v , the entropy variation σ , the pressure variation p , the density variation ρ , and the temperature variation τ . The parameters that specify the properties and nature of the fluid are the ambient values of the density ρ_0 , the static pressure P_0 , the shear viscosity coefficient μ , the bulk viscosity coefficient η , the thermal diffusivity of the enclosed gas α_t , the coefficient of thermal conductivity λ_t , the specific heat coefficient at constant pressure and constant volume per unit of mass C_p and C_v respectively, the specific heat ratio γ , and the increase in pressure per unit increase in temperature at constant density β . The complete set of linearized homogeneous equations governing small-amplitude disturbances of the fluid includes the following equations:

- The Navier–Stokes equation

$$\frac{1}{c_0} \frac{\partial v}{\partial t} + \frac{1}{\rho_0 c_0} \nabla p = \ell_v \nabla (\nabla \cdot v) - \ell'_v \nabla \times (\nabla \times v), \quad (1)$$

where ℓ_v and ℓ'_v are characteristic lengths defined as

$$\ell_v = \frac{1}{\rho_0 c_0} \left(\frac{4}{3} \mu + \eta \right) \text{ and } \ell'_v = \frac{\mu}{\rho_0 c_0}.$$

- The Fourier equation for heat conduction, taking into account the thermodynamic law expressing the entropy

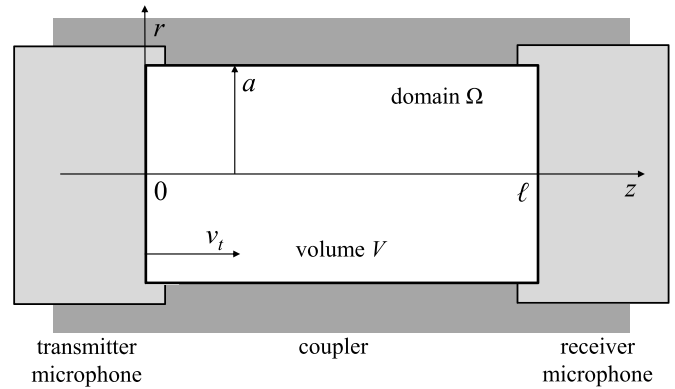


Figure 1. Coupler geometry with the two microphones.

variation σ as function of the independent variables p and τ ,

$$\left(\frac{\partial}{\partial t} - \alpha_t \nabla^2 \right) \tau = \frac{\gamma - 1}{\beta \gamma} \frac{\partial p}{\partial t}. \quad (2)$$

- The conservation of mass equation, taking into account the thermodynamic law expressing the density variation as function of the independent variable p and τ with $\rho = (p - \beta \tau) \gamma / c_0^2$,

$$\rho_0 c_0 \nabla \cdot v + \frac{\gamma}{c_0} \frac{\partial}{\partial t} (p - \beta \tau) = 0. \quad (3)$$

The acoustic pressure inside the cavity should be the solution of this set of three equations with the requirement of regular behavior at the cylinder center (the field remains finite at $r=0$) and with the boundary conditions at the surface of the domain presented hereafter when required.

Several simplifying hypothesis can be made, summarized as follows: (i) as the system has an axial symmetry, the acoustic field is assumed to be independent of the azimuthal component θ , (ii) the radial component r of the particle velocity v_r vanishes, as it is much lower than the axial component z , and thus the pressure variation p does not depend on the radial coordinate r (quasi-plane wave approximation), (iii) since the shear viscosity effects are important, the spatial derivative of the particle velocity with respect to the axial coordinate z in the Navier–Stokes equation is much smaller than the derivative with respect to the radial coordinate r .

These approximations allow us to simplify the Navier–Stokes equation (1) since only the axial component needs to be considered. It takes the following approximated form:

$$\left[\frac{1}{c_0} \frac{\partial}{\partial t} - \ell'_v \frac{1}{r} \frac{\partial}{\partial r} r \frac{\partial}{\partial r} \right] v_z(r, z) = - \frac{1}{\rho_0 c_0} \frac{\partial}{\partial z} p(z). \quad (4)$$

To this differential equation are associated the two following conditions on the particle velocity:

$$\begin{aligned} v_z \text{ remains finite at } r=0, \\ v_z(a, z) = 0, \forall z \in [0, \ell]. \end{aligned} \quad (5)$$

The solution to the set of equations (4) and (5) can be written for a harmonic motion (the factor $e^{j\omega t}$ is omitted):

$$v_z(r, z) = \frac{j}{k_0 c_0 \rho_0} \frac{\partial}{\partial z} p(z) \left[1 - \frac{J_0(k_v r)}{J_0(k_v a)} \right], \quad (6)$$

where J_0 is the 0th-order cylindrical Bessel's function of the first kind and the expressions of the wavenumber k_v (associated with the vertical movement due to viscosity effects) is given by

$$k_v = \frac{1-j}{\sqrt{2}} \sqrt{k_0/\ell'_v}, \quad (7)$$

where $k_0 = \omega/c_0$ is the adiabatic wavenumber. The average value of v_z over the section $S = \pi a^2$ of the cavity is given by

$$\begin{aligned} \langle v_z(z) \rangle_S &= \frac{2\pi}{S} \int_0^a v_z(r, z) r dr, \\ &= \frac{j}{k_0 \rho_0 c_0} \frac{\partial}{\partial z} p(z) [1 - K_v], \end{aligned} \quad (8)$$

with

$$K_v = \frac{2}{k_v a} \frac{J_1(k_v a)}{J_0(k_v a)}, \quad (9)$$

where J_1 is the 1st-order cylindrical Bessel's function of the first kind.

As no approximations are formulated for the temperature variation τ (excepting the axial symmetry of the system), the Fourier equation (2) takes the general form:

$$\left[\frac{\partial}{\partial t} - \alpha_r \left(\frac{\partial^2}{\partial z^2} + \frac{1}{r} \frac{\partial}{\partial r} r \frac{\partial}{\partial r} \right) \right] \tau(r, z, t) = \frac{\gamma - 1}{\beta \gamma} \frac{\partial p}{\partial t}. \quad (10)$$

The pressure variation is associated with a temperature variation in the fluid that is responsible for a heat transfer from the fluid to the boundaries. The resulting perturbation of the acoustic wave takes the form of attenuation due to dissipation of the thermal energy. For most applications involving solid walls, the product of the heat capacity of the wall by its thermal conductivity is significantly greater than its equivalent product for the fluid. As a result, the boundary condition on the temperature variation at the interface between the fluid and the solid walls is commonly approximated in the literature as an isothermal boundary condition [19]. It is worth noting that this approximation may require reevaluation in future work, particularly regarding low frequencies (below 1 Hz) and at boundaries featuring thin walls, such as microphone diaphragms [20]. However, this specific issue is beyond the scope of the present paper. Consequently, the following conditions on the temperature variation are associated with the differential equation (10):

$$\begin{aligned} \tau \text{ remains finite at } r = 0, \quad \forall z \in [0, \ell], \\ \tau(a, z) = 0, \quad \forall z \in [0, \ell], \\ \tau(r, 0) = 0 \text{ and } \tau(r, \ell) = 0, \quad \forall r \in [0, a]. \end{aligned} \quad (11)$$

The Fourier equation (10) subject to the boundary conditions (11) has been extensively discussed in the literature in the context of reciprocity calibration of microphones [10, 12, 13, 21]. Especially, [13] provides further details on the methodologies and assumptions used to solve this equation, which have led to the broadband and low-frequency solutions discussed above. In brief, the approach leading to the broadband solution is based on the plane wave propagation theory in infinite cylindrical tubes, where the spatial derivative of the temperature variation τ with respect the z -coordinate is neglected in the Fourier equation. Then, heat conduction effects at the end of the coupler are considered by adding thermal boundary layer admittances in the boundary conditions of the problem. This approach turns out to be inappropriate at the lower frequency range, and especially at infrasonic frequencies [12, 13]. On the other hand, the approach that leads to the low-frequency solution is based on solving the Fourier equation, as proposed by Gerber [5]. This solution assumes uniform pressure variation inside the cavity, which as expected, is not appropriate for the highest frequency range. Thus, finding an appropriate solution to the Fourier equation is crucial to achieve the objective of a unified formulation valid across a wide frequency range. For this purpose, the inhomogeneous Fourier equation (10) is solved without making the aforementioned assumptions. Specifically, the Duhamel's principle is used to convert the problem with a source to an initial value problem (see for example [22]). The detailed calculations are provided in appendix A. Then, the solution of equation (10) subject to conditions (11) takes the general form:

$$\begin{aligned} \tau(r, z) &= \frac{\gamma - 1}{\beta \gamma} \sum_{m=1}^{+\infty} \sum_{n=1}^{+\infty} \frac{4J_0(j_n r/a)}{j_n \ell J_1(j_n)} \sin\left(\frac{m\pi}{\ell} z\right) \\ &\cdot \frac{1}{1 + \frac{\alpha_r}{j\omega} \left[\left(\frac{m\pi}{\ell}\right)^2 + \left(\frac{j_n}{a}\right)^2 \right]} \int_0^\ell \sin\left(\frac{m\pi}{\ell} z\right) p(z) dz, \end{aligned} \quad (12)$$

with j_n the roots of $J_0(j_n) = 0$ and where the pressure variation $p(z)$ must remain in the integral part as long as it is assumed as non-uniform inside the cavity. The average value of $\tau(r, z)$ over the section of the cavity is given by

$$\begin{aligned} \langle \tau(z) \rangle_S &= \frac{2\pi}{S} \int_0^a \tau(r, z) r dr, \\ &= \frac{\gamma - 1}{\beta \gamma} \sum_{m=1}^{+\infty} \sum_{n=1}^{+\infty} a_{m,n} \sin\left(\frac{m\pi}{\ell} z\right) \\ &\cdot \int_0^\ell \sin\left(\frac{m\pi}{\ell} z\right) p(z) dz, \end{aligned} \quad (13)$$

where

$$a_{m,n} = \frac{8}{j_n^2 \ell} F_{m,n}, \quad (14)$$

with

$$F_{m,n} = \frac{1}{1 + \frac{\alpha_t}{j\omega} \left[\left(\frac{m\pi}{\ell} \right)^2 + \left(\frac{j\omega}{a} \right)^2 \right]}. \quad (15)$$

Taking the average value across the section of the cavity, the conservation of mass equation (3) takes the form:

$$\frac{\partial}{\partial z} \langle v_z(z) \rangle_S + \frac{j\omega}{\rho_0 c_0^2} \gamma (p(z) - \beta \langle \tau(z) \rangle_S) = 0. \quad (16)$$

Combining equations (8) and (13) with equation (16) leads to the following propagation equation along the axis of the cylindrical cavity:

$$\begin{aligned} \frac{\partial^2}{\partial z^2} p(z) &= Z_v Y_{ha} \gamma p(z) - Z_v Y_{ha} (\gamma - 1) \\ &\cdot \sum_{m=1}^{+\infty} \sum_{n=1}^{+\infty} a_{m,n} \sin \left(\frac{m\pi}{\ell} z \right) \int_0^\ell \sin \left(\frac{m\pi}{\ell} z \right) p(z) dz, \end{aligned} \quad (17)$$

where

$$Z_v = \frac{1}{S} \frac{jk_0 \rho_0 c_0}{1 - K_v}, \quad (18)$$

and

$$Y_{ha} = S \frac{jk_0}{\rho_0 c_0}. \quad (19)$$

Finally, the following boundary conditions (evoking equations (8) and (18)) are associated to the propagation equation:

$$-\frac{1}{Z_v} \frac{\partial p}{\partial z} = S v_t \quad \text{at } z = 0, \quad (20a)$$

$$\frac{1}{Z_v} \frac{\partial p}{\partial z} = -Y_r p \quad \text{at } z = \ell, \quad (20b)$$

where Y_r is the acoustic admittance of the receiver microphone.

3. Solutions for the acoustic transfer admittance

3.1. The general analytical solution

The propagation equation (17) takes the form of a linear Fredholm integro-differential equation of the second kind. The Adomian decomposition method (ADM), introduced by Adomian in the 80s [23] is a common method used to solve linear and non-linear integro-differential equations. This method generates a solution in the form of a series whose terms are determined by a recursive relation. In the present problem, the modified form of LADM [24] is particularly relevant, as it generates a solution that closely approximates the intended solution from the first iteration. Initially, equation (17) is rewritten in a form that enables easier interpretation

$$\begin{aligned} \frac{\partial^2}{\partial z^2} p(z) &= -\chi_t^2 p(z) + \alpha \sum_{m=1}^{+\infty} \sum_{n=1}^{+\infty} a_{m,n} \sin \left(\frac{m\pi}{\ell} z \right) \\ &\cdot \int_0^\ell \sin \left(\frac{m\pi}{\ell} z \right) p(z) dz, \end{aligned} \quad (21)$$

where

$$\chi_t = \sqrt{-Z_v Y_{ha} \gamma} = \frac{\omega}{c_0} \sqrt{\frac{\gamma}{1 - K_v}}, \quad (22)$$

is the ‘isothermal’ wavenumber which includes viscosity effects, and

$$\alpha = -Z_v Y_{ha} (\gamma - 1) = \chi_t^2 - \chi_a^2, \quad (23)$$

with

$$\chi_a = \sqrt{-Z_v Y_{ha}} = \frac{\omega}{c_0} \sqrt{\frac{1}{1 - K_v}}, \quad (24)$$

the ‘adiabatic’ wavenumber which includes viscosity effects.

The first step in the LADM is to apply the Laplace transform operator to the propagation equation (21), resulting in a simplified propagation equation that takes the form of an integral equation (see appendix B for details):

$$\begin{aligned} p(z) &= p(0) \cos(\chi_t z) + \frac{p'(0)}{\chi_t} \sin(\chi_t z) \\ &+ \alpha \sum_{m=1}^{+\infty} \sum_{n=1}^{+\infty} a_{m,n} \phi_m(z) \int_0^\ell \sin \left(\frac{m\pi}{\ell} z \right) p(z) dz, \end{aligned} \quad (25)$$

where $p(0)$ and $p'(0)$ are constants fixed by the boundary conditions ((20a) and (20b)) (see appendix C for details) and

$$\phi_m(z) = \frac{1}{\chi_t} \frac{\chi_t \sin \left(\frac{m\pi}{\ell} z \right) - \left(\frac{m\pi}{\ell} \right) \sin(\chi_t z)}{\chi_t^2 - \left(\frac{m\pi}{\ell} \right)^2}. \quad (26)$$

It is worth noting that the first two terms in the equation (25) represent the plane wave solution for an isothermal regime. The ADM assumes that the solution to equation (25) can be represented in the form of an infinite series given by

$$p(z) = \sum_{k=0}^{+\infty} p_k(z), \quad (27)$$

where the terms $p_k(z)$ are calculated recursively. Then, these terms $p_k(z)$ are given by (see appendix B for details)

$$p_0(z) = p(0) \cos(\chi_t z) + \frac{p'(0)}{\chi_t} \sin(\chi_t z), \quad (28)$$

for $k = 0$, and

$$\begin{aligned} p_k(z) &= p(0) \alpha^k \sum_{m=1}^{+\infty} \sum_{n=1}^{+\infty} a_{m,n} \phi_m(z) \beta_{k,m} \\ &+ \frac{p'(0)}{\chi_t} \alpha^k \sum_{m=1}^{+\infty} \sum_{n=1}^{+\infty} a_{m,n} \phi_m(z) \beta'_{k,m}, \end{aligned} \quad (29)$$

for $k \geq 1$ where

$$\beta_{k,m} = \sum_{\nu=1}^{+\infty} \sum_{\mu=1}^{+\infty} a_{\nu,\mu} \beta_{k-1,\nu} \psi_{m,\nu}, \quad (30a)$$

$$\beta'_{k,m} = \sum_{\nu=1}^{+\infty} \sum_{\mu=1}^{+\infty} a'_{\nu,\mu} \beta'_{k-1,\nu} \psi_{m,\nu}, \quad (30b)$$

are the recursive relations, the first terms being given by

$$\beta_{1,m} = \frac{\frac{m\pi}{\ell} ((-1)^m \cos(\chi_t \ell) - 1)}{\chi_t^2 - \left(\frac{m\pi}{\ell}\right)^2}, \quad (31a)$$

$$\beta'_{1,m} = \frac{\frac{m\pi}{\ell} (-1)^m \sin(\chi_t \ell)}{\chi_t^2 - \left(\frac{m\pi}{\ell}\right)^2}, \quad (31b)$$

and where

$$\psi_{m,\nu} = \delta_{m,\nu} \frac{\ell/2}{\chi_t^2 - \left(\frac{m\pi}{\ell}\right)^2} - \frac{\frac{1}{\chi_t} \frac{m\pi}{\ell} \frac{\nu\pi}{\ell} (-1)^m \sin(\chi_t \ell)}{\left(\chi_t^2 - \left(\frac{\nu\pi}{\ell}\right)^2\right) \left(\chi_t^2 - \left(\frac{m\pi}{\ell}\right)^2\right)}, \quad (32)$$

with $\delta_{m,\nu}$ the Kronecker delta.

As mentioned in the introduction, the quantity of interest for the pressure reciprocity calibration method is the acoustic transfer admittance Y_T defined as the quotient of the short-circuit volume velocity produced by the microphone used as a transmitter by the sound pressure acting on the diaphragm of the microphone used as a receiver [1], namely

$$Y_T = \frac{Sv_t - Y_t p(0)}{p(\ell)}, \quad (33)$$

where Y_t is the acoustic admittance of the transmitting microphone. By invoking equations (C.5) and (C.7) for $p(0)$ and $p(\ell)$ respectively, the acoustic transfer admittance takes the following form for the general analytical solution

$$Y_T = - \left(\frac{\chi_t}{Z_v} - Y_t \frac{C_0 + Z_v Y_r D_0}{A_0 + Z_v Y_r B_0} \right) \cdot \left(D_0 - B_0 \frac{C_0 + Z_v Y_r D_0}{A_0 + Z_v Y_r B_0} \right)^{-1}, \quad (34)$$

where the constants A_0 , B_0 , C_0 and D_0 are given by (C.6a), (C.6b), (C.6c) and (C.6d) respectively.

The differences between the acoustic transfer admittances derived from the IEC standards [1, 17] (i.e. the low-frequency solution, the extended low-frequency solution and the broadband solution) in comparison to the general analytical solution (34) are presented in figures 2 and 3. These results are presented for the dimensions of common LS1 and LS2 plane-wave couplers specified in table 1. In these numerical results, the acoustic admittances of the microphones were calculated using a lumped parameter model as described in [1], considering the nominal parameters of LS B&K microphones

specified in table 2. Note that this model for the acoustic admittances of the microphones does not take into account heat conduction effects in the cavity behind the diaphragm of microphones. These effects could significantly contribute to the reciprocity calibration results at lower frequencies, typically below 2 Hz [9, 15]. However, these effects do not really matter when the purpose is to compare models of acoustic transfer admittances of cylindrical cavities, with the same acoustic admittances of the microphones in each case. Thus, the numerical results presented in the figures clearly show the equivalences of the general analytical solution (34) with the standardized models. These equivalences are observed within the frequency ranges where the standardized models are considered valid, namely (i) at low frequencies for the low-frequency solution, (ii) at low and mid frequencies for the extended low-frequency solution, and (iii) at mid and high frequencies for the broadband solution. This provides evidence supporting the validity of the general analytical solution as a unified formulation of the acoustic transfer admittance. Note that the low-frequency solutions remain equivalent despite not being presented for frequencies below 0.1 Hz. Small deviations are observed specifically at the axial resonance frequencies of the couplers, i.e. the region above 10 kHz. It is important to mention that these differences are several orders of magnitude smaller than the measurement uncertainty at these frequencies. As the closed tube system is underdamped, the acoustic transfer admittance is highly sensitive to input parameters at resonance frequencies. Thus, inherent differences in the models being compared can account for these deviations. For example, the broadband model in the IEC standard makes use of ‘large tube’ asymptotic approximations for both the propagation constant and the characteristic admittance, whereas these approximations are not used in the present model. Note that the finite calculation of the three sums ($N_k, N_{m,\nu}, N_{n,\mu}$) in equations (27), (29), (30a) and (30b) does not contribute to these deviations, as the values ($N_k, N_{m,\nu}, N_{n,\mu}$) were chosen large enough to ensure the convergence of the solution.

The figure 4 presents an example of convergence study for a LS1 coupler ($\ell = 18.9$ mm), i.e. the number of iterations ($N_k, N_{m,\nu}, N_{n,\mu}$) required as function of frequency for the convergence of the acoustic transfer admittance within a tolerance of 0.001 dB for the amplitude and 0.01 degree for the phase. At 2 Hz, the study shows the expected results with ($N_k, N_{m,\nu}, N_{n,\mu}$) = (1,20,14) and increasing significantly with frequency, reaching ($N_k, N_{m,\nu}, N_{n,\mu}$) = (10,1600,1000) at 30 kHz. It is worth noting that the calculation of the solution can require substantial power computing resources, essentially due to the nested double sum in the recursive equations (29), (30a) and (30b). However, these resources can be optimized firstly by implementing a frequency dependence of the number of iterations required to converge to an accurate solution. The convergence study suggests that utilizing the frequency dependencies $N_k = \lceil 0.2f^{0.42} \rceil$, $N_{m,\nu} = \lceil 30f^{0.42} \rceil$ and $N_{n,\mu} = \lceil 15f^{0.42} \rceil$ is effective in achieving a solution within a tolerance of 0.001 dB for the amplitude and 0.01 degree for the phase. In addition, notable enhancements in the perform-

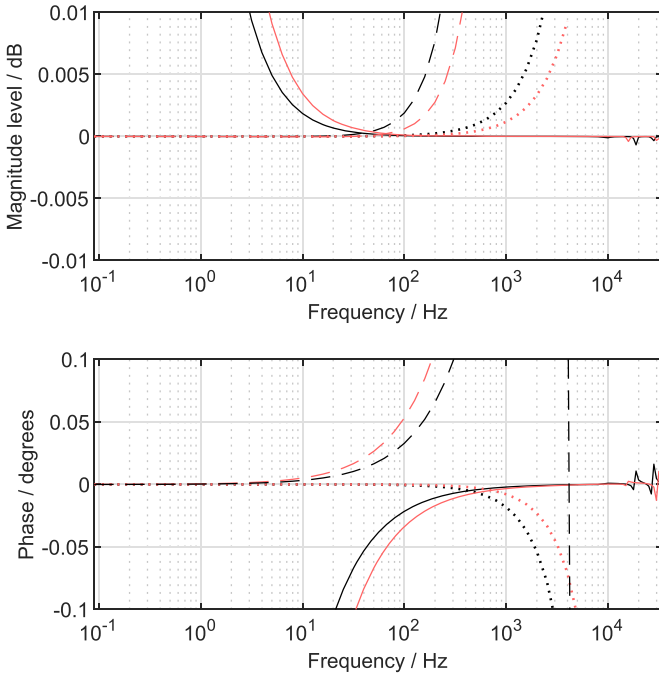


Figure 2. Difference for the magnitude level in dB (upper graph) and phase in degrees (lower graph) between the acoustic transfer admittances derived from the IEC models (broken lines: low-frequency solution, dotted lines: extended low-frequency solution and solid lines: broadband solution) in comparison to the general analytical solution (34), for LS1 couplers $a = 9.3$ mm, $\ell = 11.4$ mm (red curves) and $\ell = 18.9$ mm (black curves). The results presented for the two low-frequency models are limited to frequencies below 5 kHz.

ance of the algorithm can be achieved by focusing on efficient memory allocation, especially when considering relevant pre-processing calculations. Thus, when using such an optimized algorithm, the solution can be calculated in just a few seconds for a typical frequency range covering 1/3 octave frequencies between 2 Hz and 25 kHz. An example of Python code that has been optimized in this way is provided as supplementary material.

3.2. The general semi-analytical numerical solution

This section provides an alternative method based on a numerical technique to solve the problem addressed in section 2. The technique consists of a stepped duct approximation where short discs of width $\Delta\ell$ are considered, and the sound pressure within them can be assumed to be uniform, $p(z_i) \approx p(z_i + \Delta\ell)$. This approximation allows in particular to extract the sound pressure $p(z)$ from the integral part in the solution of the Fourier equation (13). Thus, the integral part in that equation applies to a simple sine function, straightforwardly calculable as

$$\int_0^\ell \sin\left(\frac{m\pi}{\ell}z\right) dz = \frac{\ell}{m\pi} [1 - (-1)^m].$$

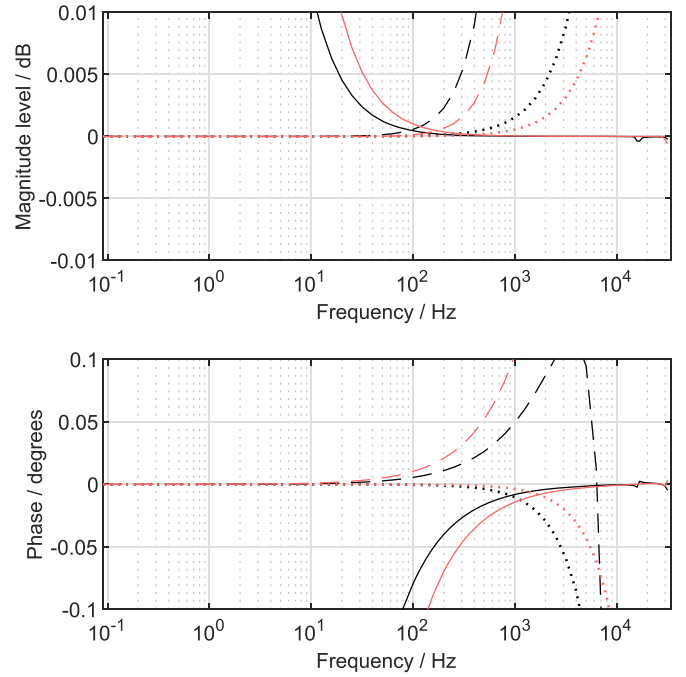


Figure 3. Difference for the magnitude level in dB (upper graph) and phase in degrees (lower graph) between the acoustic transfer admittances derived from the IEC models (broken lines: low-frequency solution, dotted lines: extended low-frequency solution and solid lines: broadband solution) in comparison to the general analytical solution (34), for LS2 couplers $a = 4.65$ mm, $\ell = 5.7$ mm (red curves) and $\ell = 10.4$ mm (black curves). The results presented for the two low-frequency models are limited to frequencies below 10 kHz.

Table 1. Plane-wave coupler parameters (the lengths include the front cavity depth of the two LS microphones).

| Parameters | LS1 microphones | | LS2 microphones | |
|----------------|-------------------|---------|-----------------|---------|
| | Length (ℓ) | 18.9 mm | 11.4 mm | 10.4 mm |
| Radius (a) | 9.3 mm | 9.3 mm | 4.65 mm | 4.65 mm |

Table 2. Microphone parameters.

| Parameters | LS1 | LS2 |
|---------------------|---------------------|---------------------|
| | B&K Type 4160 | B&K Type 4180 |
| Equivalent Volume | 148 mm ³ | 9.3 mm ³ |
| Resonance frequency | 8500 Hz | 23 000 Hz |
| Loss factor | 1.08 | 1.05 |

Noting that the previous integral is equal to zero for even m terms, the solution (13) of the Fourier equation is locally given by

$$\langle \tau(z) \rangle_S = p(z) \frac{\gamma - 1}{\beta\gamma} E_p(z), \quad \forall z \in [z_i, z_i + \Delta\ell], \quad (35)$$

where

$$E_p(z) = \sum_{m=0}^{+\infty} \sum_{n=1}^{+\infty} b_{m,n} \sin\left(\frac{(2m+1)\pi}{\ell}z\right), \quad (36)$$

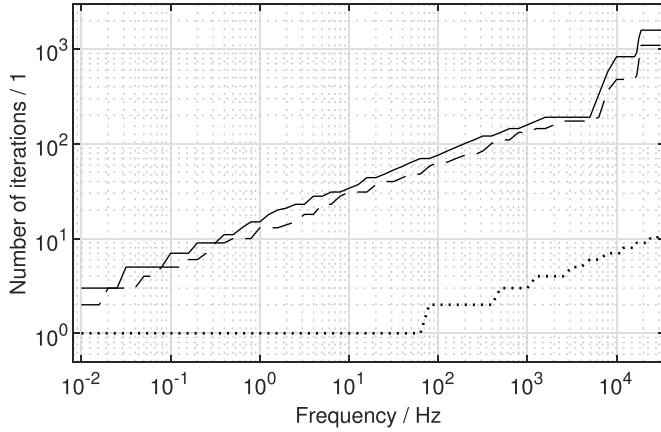


Figure 4. Number of iterations ($N_k, N_{m,\nu}, N_{n,\mu}$) as function of frequency required for the convergence within a tolerance of 0.001 dB for the amplitude and 0.01 degree for the phase of the acoustic transfer admittance, for a LS1 coupler $\ell = 18.9$ mm and $a = 9.3$ mm. (a) dotted line: N_k terms required in (27) for the isothermal to adiabatic correction, (b) solid line: $N_{m,\nu}$ terms required for the axial eigenvalues and (c) broken line: $N_{n,\mu}$ terms required for the radial eigenvalues.

and (evoking equation (14))

$$b_{m,n} = \frac{8/\pi}{(m+1/2)j_n^2} F_{2m+1,n}, \quad (37)$$

where $F_{2m+1,n}$ is given by (15) with m replaced by $2m+1$. For a short width $\Delta\ell$, the function $E_p(z)$ with $z \in [z_i, z_i + \Delta\ell]$ can be approximated by its average value across $\Delta\ell$ as

$$\begin{aligned} E_p(z) &\approx \langle E_p(z_i) \rangle_{\Delta\ell} = \frac{1}{\Delta\ell} \int_{z_i}^{z_i+\Delta\ell} E_p(z) dz \\ &= \frac{\ell}{\Delta\ell} \sum_{m=0}^{+\infty} \sum_{n=1}^{+\infty} b_{m,n} \left(\frac{\cos\left(\frac{(2m+1)\pi}{\ell} z_i\right)}{(2m+1)\pi} \right. \\ &\quad \left. - \frac{\cos\left(\frac{(2m+1)\pi}{\ell} (z_i + \Delta\ell)\right)}{(2m+1)\pi} \right). \end{aligned} \quad (38)$$

Therefore, combining equations (8), (35) and (38) with equation (16) to remove the variable $\langle \tau(z) \rangle_S$, denoting $w(z) = S \langle v_z(z) \rangle_S$ the axial acoustic volume velocity, leads to the pair of equations:

$$\frac{\partial}{\partial z} p(z) + Z_v w(z) = 0, \quad \forall z \in [z_i, z_i + \Delta\ell], \quad (39a)$$

$$\frac{\partial}{\partial z} w(z) + Y_h(z_i) p(z) = 0, \quad \forall z \in [z_i, z_i + \Delta\ell], \quad (39b)$$

where the impedance Z_v is given by equation (18) and the admittance $Y_h(z_i)$ is locally a constant at $z \in [z_i, z_i + \Delta\ell]$, given by

$$Y_h(z_i) = S \frac{j k_0}{\rho_0 c_0} \Delta_H(z_i), \quad (40)$$

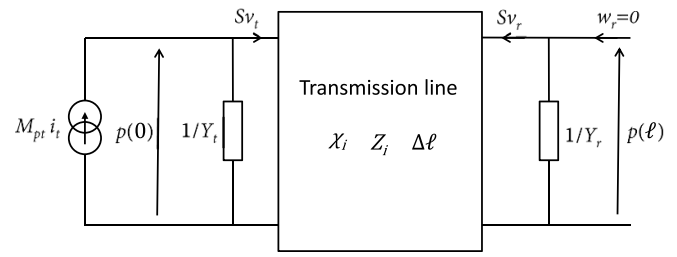


Figure 5. Two-port transmission line model of the complete reciprocity system, consisting of the two microphones and the coupling cavity.

with

$$\Delta_H(z_i) = \gamma - (\gamma - 1) \langle E_p(z_i) \rangle_{\Delta\ell}. \quad (41)$$

Note the notation used above is chosen to be similar to the one commonly used in the community involved in reciprocity calibration of microphones [1, 17].

The set of equations (39a) and (39b) takes the form of the usual pair of transmission line equations which can be represented as a two-port network. Thus, for a length $\Delta\ell$ of uniform transmission line, the interrelated relationships between the sound pressure and volume velocity are given by the usual $ABCD$ parameters matrix (see for example [25])

$$\begin{bmatrix} p(z_i) \\ w(z_i) \end{bmatrix} = \begin{bmatrix} A_i & B_i \\ C_i & D_i \end{bmatrix} \cdot \begin{bmatrix} p(z_i + \Delta\ell) \\ w(z_i + \Delta\ell) \end{bmatrix}. \quad (42)$$

with (the hyperbolic notation is preferred here to align with the notation used in IEC 61 094-2 [1])

$$\begin{bmatrix} A_i & B_i \\ C_i & D_i \end{bmatrix} = \begin{bmatrix} \cosh(\chi_i(z_i)\Delta\ell) & \frac{1}{Y_i(z_i)} \sinh(\chi_i(z_i)\Delta\ell) \\ Y_i(z_i) \sinh(\chi_i(z_i)\Delta\ell) & \cosh(\chi_i(z_i)\Delta\ell) \end{bmatrix}, \quad (43)$$

where

$$\chi_i(z_i) = j \sqrt{-Z_v Y_h(z_i)} = j \frac{\omega}{c_0} \sqrt{\frac{\Delta_H(z_i)}{1 - K_v}}, \quad (44)$$

is the complex propagation constant and

$$Y_i(z_i) = \sqrt{\frac{Y_h(z_i)}{Z_v}} = \frac{S}{\rho_0 c_0} \sqrt{(1 - K_v) \Delta_H(z_i)}, \quad (45)$$

is the characteristic admittance, both locally constants in $z \in [z_i, z_i + \Delta\ell]$. For the complete system, consisting of the two microphones and the coupling cavity, the equivalent model for which is shown in figure 5, the matrix chain of the two-port network takes the form

$$\begin{bmatrix} p(0) \\ S v_t \end{bmatrix} = \begin{bmatrix} A & B \\ C & D \end{bmatrix} \cdot \begin{bmatrix} 1 & 0 \\ Y_r & 1 \end{bmatrix} \cdot \begin{bmatrix} p(\ell) \\ -w_r = 0 \end{bmatrix}, \quad (46)$$

with

$$\begin{bmatrix} A & B \\ C & D \end{bmatrix} = \prod_{i=0}^{N-1} \begin{bmatrix} A_i & B_i \\ C_i & D_i \end{bmatrix}, \quad (47)$$

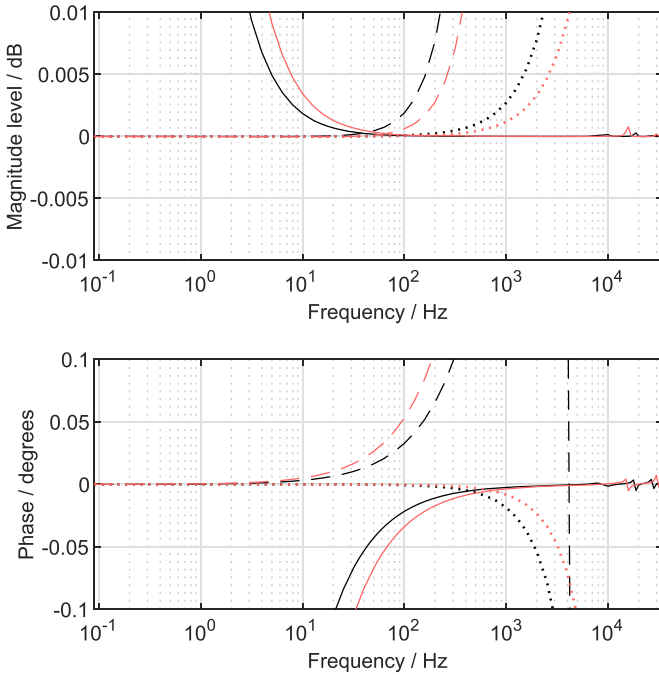


Figure 6. Difference for the magnitude level in dB (upper graph) and phase in degrees (lower graph) between the acoustic transfer admittances derived from the IEC models (broken lines: low-frequency solution, dotted lines: extended low-frequency solution and solid lines: broadband solution) in comparison to the general semi-analytical numerical solution (49), for LS1 couplers $a = 9.3$ mm, $\ell = 11.4$ mm (red curves) and $\ell = 18.9$ mm (black curves). The results presented for the two low-frequency models are limited to frequencies below 5 kHz.

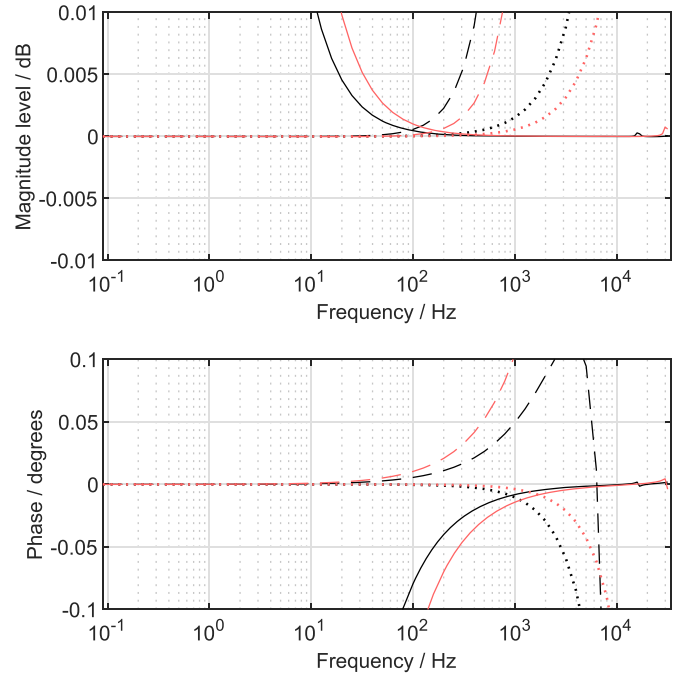


Figure 7. Difference for the magnitude level in dB (upper graph) and phase in degrees (lower graph) between the acoustic transfer admittances derived from the IEC models (broken lines: low-frequency solution, dotted lines: extended low-frequency solution and solid lines: broadband solution) in comparison to the general semi-analytical numerical solution (49), for LS2 couplers $a = 4.65$ mm, $\ell = 5.7$ mm (red curves) and $\ell = 10.4$ mm (black curves). The results presented for the two low-frequency models are limited to frequencies below 10 kHz.

where N is the number of segments of width $\Delta\ell$ considered to mesh the axial dimension of the cavity. Thus, from equation (46) the two following equations can be provided

$$p(0) = (A + Y_r \cdot B)p(\ell), \quad (48a)$$

$$Sv_t = (C + Y_r \cdot D)p(\ell). \quad (48b)$$

Finally, combining the set of equations (48a) and (48b) with (33) leads to the following form for the acoustic transfer admittance of the cavity

$$Y_T = C + Y_r D + Y_r A + Y_r Y_t B. \quad (49)$$

Similarly to the results presented in the previous section, the differences between the acoustic transfer admittances derived from the three IEC standards [1, 17] and the general semi-analytical numerical solution (49) are presented in figures 6 and 7. These results are presented for the dimensions of the LS1 and LS2 plane-wave couplers specified in table 1. These comparisons indicate that the general semi-analytical numerical solution (49) is equivalent to the standardized models within the frequency ranges where they are

considered valid. This provides evidence supporting the validity of the general semi-analytical numerical solution as a unified formulation of the acoustic transfer admittance. The small deviations observed at high frequencies, particularly at the axial resonance frequencies of the coupler, are also attributed here to the inherent differences in the models being compared. Note that the finite calculation of the double sum (N_m, N_n) in equation (38), and the finite meshing considered in the transmission line matrix (47) do not contribute to the deviations, as the values were chosen large enough to ensure the convergence of the solution. Here, for the large LS1 coupler, the number of terms (N_m, N_n) required to converge to a solution within a tolerance of 0.001 dB and 0.01 degree are $(N_m, N_n) = (10, 14)$ at 2 Hz, increasing significantly with frequency to reach $(N_m, N_n) = (800, 1000)$ at 30 kHz. The meshing of the axial dimension of the cavity requires special attention due to the stepped duct approximation. In particular, two factors must be considered: (i) the assumption of uniform sound pressure in a slice of duct, where its variation increases with frequency. This requires a finer meshing at higher frequencies to accurately model the acoustic behavior, and (ii) the assumption of averaging the function $\langle E_p(z_i) \rangle_{\Delta\ell}$ across the width $\Delta\ell$ of a slice of duct, where its variation increases near the thermal boundary layers at $z = 0$ and $z = \ell$ due to the isothermal boundary condition $\tau = 0$ (see figure 8). In this multiscale problem, the mesh must be refined where needed,

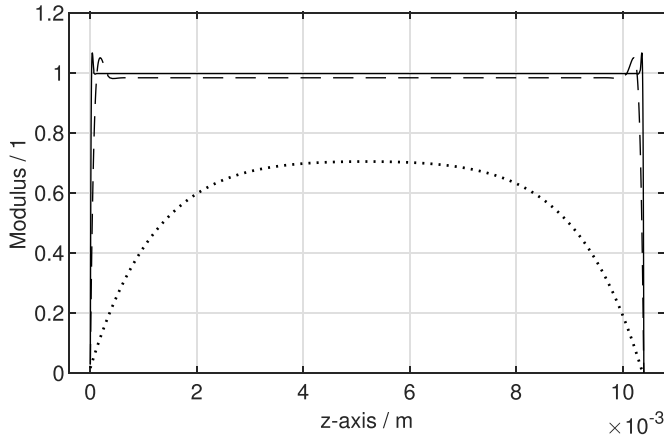


Figure 8. Modulus of the function $E_p(z)$ at 2 Hz (dotted line), 1 kHz (broken line) and 25.1 kHz (solid line) as function of the z -axis for a LS2 coupler, $\ell = 10.4$ mm and $a = 4.65$ mm.

which is a non-trivial task because the boundary layer thickness varies with frequency. In the bulk of the domain, the field is smooth and varies with the acoustic wavelength, which is larger by several order of magnitude than the thermal boundary layer thickness given by

$$\delta_h = \sqrt{\frac{2\alpha_t}{\omega}}. \quad (50)$$

Using an anisotropic mesh with a finer width $\Delta\ell$ near the boundaries ends of the cavity is of interest here. This approach reduces errors in the solution by using fine meshing exactly where it is needed, while simultaneously conserving computing resources. To calculate the results presented in figures 6 and 7, the bulk of the domain was meshed with a minimum of ten elements ($N = 10$), which increases as function of frequency according to the formula $N = \lceil 10\ell\omega/c_0 \rceil$ (equivalent to ten elements per wavelength). At the ends of the cavity, the domain width, delimited by four times the thermal boundary layer thickness δ_h , was meshed with ten elements. This basic parameterization is sufficient to calculate a solution within a tolerance of 0.001 dB and 0.01 degrees at 1/3 octave frequencies between 2 Hz and 25 kHz in just a few seconds. An example of Python code for the calculation of the acoustic transfer admittance is provided as supplementary material. Finally, the level of agreement between the general semi-analytical numerical solution (49) and the general analytical solution (34) is approximately 10^{-6} dB for the amplitude and 10^{-4} degrees for the phase across a wide frequency range when using the parameterizations of the models presented above. At the axial resonance frequencies of the couplers, the level of agreement reaches maximums of 10^{-4} dB for the amplitude and 10^{-3} degrees for the phase.

3.3. The simplified analytical solution

The results presented in the previous sections provide evidence to support the validity of the two solutions proposed in this paper for covering the complete frequency range of interest for

pressure reciprocity calibrations of microphones. The fundamental equations of the problem having been established, this final section is dedicated to analyzing the extent of a simplified solution, based on similar assumptions that led to establishing the extended low-frequency solution implemented in the IEC standard 61 094-2:2009/AMD1:2022 [17]. As mentioned in the introduction, the extended low-frequency solution, motivated by the work in [14] uses the transmission line model, i.e. equation (4) of IEC 61 094-2 [1] as the framework for the solution. Then, based on observations of numerical results, the author highlights that accurate solutions can be obtained at low and medium frequencies when the correction factor Δ_H (equation (A.1) of [17]) is applied to the cross-sectional area, S in the characteristic admittance $Y_{a,0} = S/(\rho_0 c_0)$ and when the propagation constant is fixed to $k = 0 + j\omega/c_0$.

It is important to note that the correction factor Δ_H , as given by equation (A.1) in [17], is derived from one of the two solutions for the Fourier equation provided by Gerber in [5]. Recently, it has been clarified in [13] that of the two solutions given by Gerber, the one appropriate for pressure reciprocity calibrations is

$$\Delta_H = \gamma - (\gamma - 1)E_p, \quad (51)$$

where E_p is a complex quantity, given by equation (A.2) in [17] for a cylindrical cavity. Note that E_p is provided by Gerber in [5] by assuming a uniform sound pressure within the cavity and by averaging the temperature variation τ over the volume of the cavity, neglecting the local dependencies between the temperature variation and the sound pressure. While these assumptions are suitable for models at low frequencies where the sound pressure can be considered uniform in the coupler as in [5, 13, 15], the general solution (13) presented in this paper for the Fourier equation (10) demonstrates a more intricate relationship between temperature variation and sound pressure, indicating that these assumptions may not hold when dealing with high frequencies. On the other hand, the decreasing effects of heat conduction losses with increasing frequency on the sound pressure solution could mitigate the impact of such inappropriate assumptions in the Fourier equation.

Hereafter, we intend to study non-homogeneous simplifying assumptions on the fundamental equations presented in section 2. Specifically, in the Fourier equation, the pressure variation is assumed to depend only on the average of the temperature variation across the volume, and the pressure variation is assumed to be uniform within the cavity. However, these assumptions do not apply to the Navier–Stokes equation. The uniform sound pressure assumption within the cavity allows, similarly to equation (35), to extract the sound pressure $p(z)$ from the integral part in equation (12). Thus, the averaged value of τ across the volume of the cavity is given by

$$\bar{\tau} = \langle \tau \rangle_V \approx p(z) \frac{\gamma - 1}{\beta\gamma} E_p, \quad (52)$$

with

$$E_p = \sum_{m=0}^{+\infty} \sum_{n=1}^{+\infty} \frac{8/\pi^2}{(m + 1/2)^2 j_n^2} F_{2m+1,n}, \quad (53)$$

where $F_{2m+1,n}$ is given by (15) with m replaced by $2m + 1$. Note that the set of equations (15), (52) and (53) are equivalent to equations (A.1), (A.2) and (A.3) provided in [17]. Therefore, similarly to the demonstration provided in the previous section, combining equations (8) and (52) with equation (16) to remove the variable τ , the simplified pair of transmission line equations are given by

$$\frac{\partial}{\partial z} p(z) + Z_v w(z) = 0, \quad \forall z \in [0, \ell], \quad (54a)$$

$$\frac{\partial}{\partial z} w(z) + Y_{ha} \Delta_H p(z) = 0, \quad \forall z \in [0, \ell], \quad (54b)$$

where the impedance Z_v , the admittance Y_{ha} and the correction factor Δ_H are respectively given by equations (18), (19) and (51). In the context of this simplified problem, the matrix chain representing the two-port network takes the form

$$\begin{bmatrix} p(0) \\ Sv_t \end{bmatrix} = \begin{bmatrix} \cosh(\chi_s \ell) & \frac{1}{Y_s} \sinh(\chi_s \ell) \\ Y_s \sinh(\chi_s \ell) & \cosh(\chi_s \ell) \end{bmatrix} \cdot \begin{bmatrix} 1 & 0 \\ Y_r & 1 \end{bmatrix} \cdot \begin{bmatrix} p(\ell) \\ -w_r = 0 \end{bmatrix}, \quad (55)$$

where the complex propagation constant is given by

$$\chi_s = j \sqrt{-Z_v Y_{ha} \Delta_H} = j \frac{\omega}{c_0} \sqrt{\frac{\Delta_H}{1 - K_v}}, \quad (56)$$

and the characteristic admittance

$$Y_s = \sqrt{\frac{Y_{ha} \Delta_H}{Z_v}} = \frac{S}{\rho_0 c_0} \sqrt{(1 - K_v) \Delta_H}. \quad (57)$$

Equations (56) and (57) reveal a discrepancy in the application of the corrective factor Δ_H , as compared to the guidelines outlined in IEC standard 61 094-2:2009/AMD1:2022. At first, equation (57) suggests that the cross-sectional area S in the characteristic admittance needs to be corrected using $\sqrt{\Delta_H}$ instead of Δ_H . Furthermore, equation (56) reveals that the correction factor $\sqrt{\Delta_H}$ should be applied to the complex propagation constant, while the standard prescribes the use of the adiabatic propagation constant $j\omega/c_0$. Finally, the correction of both the propagation constant and the characteristic admittance by the factor $1/\sqrt{(1 - K_v)}$ and $\sqrt{(1 - K_v)}$ respectively, allows to retain the information of viscosity losses in the model, which could improve the solution, especially at medium and high frequencies.

Thus, from equation (55) the two following equations can be provided

$$p(0) = \left(\cosh(\chi_s \ell) + \frac{Y_r}{Y_s} \sinh(\chi_s \ell) \right) p(\ell), \quad (58a)$$

$$Sv_t = (Y_s \sinh(\chi_s \ell) + Y_r \cosh(\chi_s \ell)) p(\ell). \quad (58b)$$

Finally, combining the set of equations (58a) and (58b) with (33) leads to the well known form (as provided in [1]) for the acoustic transfer admittance

$$Y_T = (Y_r + Y_t) \cosh(\chi_s \ell) + Y_s \left(1 + \frac{Y_t Y_r}{Y_s^2} \right) \sinh(\chi_s \ell). \quad (59)$$

For the comparisons mentioned hereafter, the general analytical solution (34) is considered as the reference solution. The differences between the acoustic transfer admittances derived from equation (59) and the IEC extended low-frequency solution, in comparison to the reference solution are presented in figures 9 and 10. These results are presented for the plane-wave couplers specified in table 1. The figures clearly show the equivalences of the solution at low and medium frequencies. Note that the solutions remain equivalents despite not being presented for frequencies below 100 Hz. Moreover, it can be observed that using equation (59) to calculate the acoustic transfer admittance results in lower deviations at high frequencies compared to the IEC extended low-frequency solution. Therefore, the validity of the solution is extended by a few kilohertz. It essentially deviates from the reference solution near the axial resonance frequencies of the coupler, which was expected, due to the simplifying assumptions made to solve the Fourier equation. These deviations should be evaluated in relation to the measurement uncertainty in order to define the usable frequency range for the given solution. It should be noted that the use of short couplers is of particular interest here, as the resonance frequencies shift to higher frequencies as the length of the coupler decreases.

4. Conclusion

The IEC standard 61 094-2 [1] and its recent amendment [17] establish the principle for pressure calibration of LS microphones using the reciprocity technique. Calculation of the acoustic transfer admittance is a key aspect of microphone pressure reciprocity calibration. Three models are currently provided in the IEC standards for calculating the acoustic transfer admittance of cylindrical cavities and it is established that neither of these models is correct for all frequencies routinely considered in many NMIs, namely from 2 Hz to 25 kHz. In fact, there is only just a frequency range where low and high frequency models can be considered reasonably accurate so that a transition must be made.

Based on the fundamental equations of acoustics in thermoviscous fluids, this paper is intended to provide a unified formulation for the acoustic transfer admittance of cylindrical cavities, which is relevant for reciprocity calibration of LS microphones across a wide frequency range. For this purpose, the problem is considered using the common quasi-plane wave approximation, whereby the quantities are averaged over the radial axis of the cavity, thereby eliminating the dependence on radial coordinates. This paper specifically provides a new solution for the Fourier equation that is not restricted by the usual assumption of uniform pressure within the cavity. Thus, the integration of this solution and the solution of the Navier–Stokes equation in the conservation of mass equation leads to a new propagation equation, expressed as a linear Fredholm integro-differential equation of the second kind. The LADM is utilized to solve this equation, resulting in a solution in the form of a series whose terms are determined by a recursive relation. Moreover, a semi-analytical numerical technique

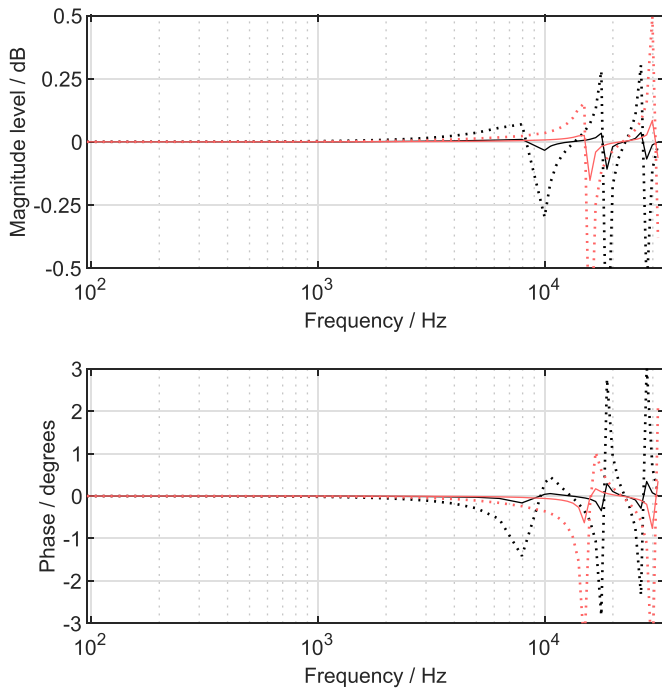


Figure 9. Difference for the magnitude level in dB (upper graph) and phase in degrees (lower graph) between the acoustic transfer admittances derived from equation (59) (solid line), the IEC extended low-frequency solution (34) (dotted line) in comparison to the general analytical solution (34), for LS1 couplers $a = 9.3$ mm, $\ell = 11.4$ mm (red curves) and $\ell = 18.9$ mm (black curves).

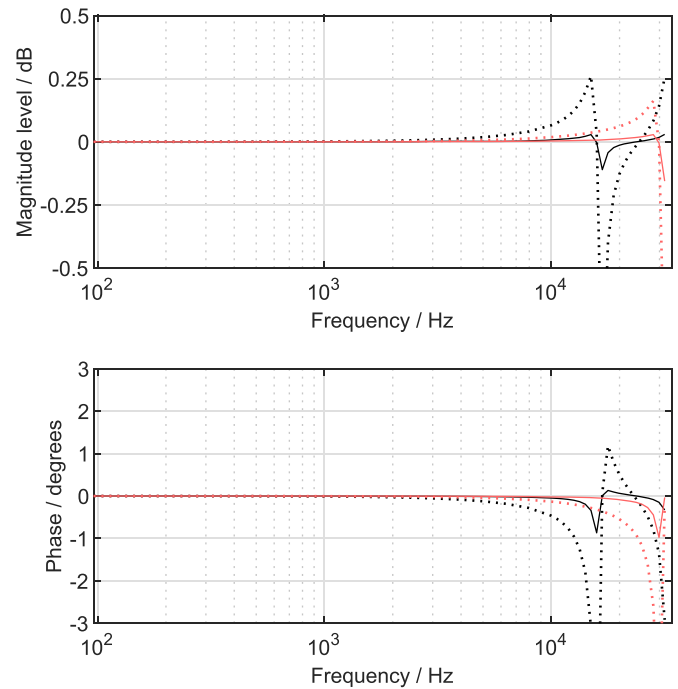


Figure 10. Difference for the magnitude level in dB (upper graph) and phase in degrees (lower graph) between the acoustic transfer admittances derived from equation (59) (solid line), the IEC extended low-frequency solution (34) (dotted line) in comparison to the general analytical solution (34), for LS2 couplers $a = 4.65$ mm, $\ell = 5.7$ mm (red curves) and $\ell = 10.4$ mm (black curves).

is used to solve the same problem. The technique involves a stepped duct approximation, where the problem is locally solved as a transmission line problem. Consequently, the entire system, comprising the two microphones and the coupling cavity, is evaluated using a matrix chain of the equivalent two-port network. The numerical results provide evidence supporting the validity of these formulations as unified formulations that covers the targeted frequency range for pressure reciprocity calibration of LS microphones. A high level of agreement is observed between the two models, approximately 10^{-6} dB for the amplitude and 10^{-4} degrees for the phase across a wide frequency range when using the parameterizations of the models presented in this paper. At the axial resonance frequencies of the couplers, the level of agreement reaches maximums of 10^{-4} dB for the amplitude and 10^{-3} degrees for the phase.

Finally, this paper evaluates the compatibility of the extended low-frequency solution provided in the IEC standard with the fundamental equations established in this study. To achieve such a formulation, non-homogeneous simplifying assumptions are considered for the Fourier and Navier–Stokes equations. Specifically, in the Fourier equation, the pressure variation is assumed to depend only on the average of the temperature variation across the volume, neglecting local dependencies, and the pressure variation is assumed to be uniform within the cavity. These assumptions, however, do not apply to the Navier–Stokes equation. This methodology leads to a solution highlighting discrepancies in the application of the corrective factor Δ_H , as compared to the guidelines outlined in amendment 1 of the standard IEC 61 094-2 [17]. Furthermore,

the obtained solution indicates how applying the corrective factor relative to viscous effects to improve the solution, particularly at high frequencies. In fact, the results presented in this paper offer numerical evidence that the solution proposed can be extended to higher frequencies. This kind of simplified analytical solution may be useful in many applications that deal with low and medium frequencies. However, incorporating non-homogeneous simplifying assumptions in the fundamental equations generates a model where restrictions are challenging to define. Thus, the validity of such a model must be assessed in relation to the measurement uncertainty, using the more rigorous solutions presented in this paper.

The primary objective of this work is to provide a unified formulation of the acoustic transfer admittance of cylindrical cavities for calibration of LS microphones by using the reciprocity technique. However, its applicability can be expanded to other calibration methods involving acoustic admittances of cylindrical cavities, as for example the calculable piston-phone [15, 26]. It is relevant to note also that the matter of radial wave motion is not discussed here. However, at high frequencies, their influence is not negligible in the calibration process, compared to the calibration uncertainties [18]. The radial wave motion results in a non-uniform pressure distribution over the microphone diaphragm, deviating from the quasi plane wave assumption made in this paper. At the highest frequencies, radial wave motion can never be avoided but can be corrected as suggested in the IEC standard 61 094-2 [1]. These corrections essentially rely on the works provided in the [18, 21], which take the form of analytical expressions based

on the assumption that the displacement function of the microphone diaphragms corresponds to idealized movements of the microphone diaphragms or on empirical data. It is accepted in the community involved in reciprocity calibration of microphones that the reliability of these corrections needs to be consolidated with further work [14]. However, given the current state of the art, the same methodology routinely applied can be used to correct radial wave motion in the models presented in this paper.

Appendix A. Solution of the inhomogeneous Fourier equation

The system defined by the inhomogeneous Fourier equation (10) subject to the boundary conditions (11) can be expressed as following:

$$\begin{cases} \left(\frac{\partial}{\partial t} - \alpha_t \nabla^2\right) \tau(r, z, t) = \Phi(z, t), \forall (r, z) \in \Omega, t > 0, \\ \tau \text{ remains finite at } r = 0, \\ \tau(a, z, t) = 0, \quad \forall z \in [0, \ell], t > 0, \\ \tau(r, 0, t) = 0 \text{ and } \tau(r, \ell, t) = 0, \quad \forall r \in [0, a], t > 0, \\ \tau(r, z, 0) = 0, \quad \forall (r, z) \in \Omega, t = 0, \end{cases} \quad (\text{A.1})$$

where

$$\Phi(z, t) = \frac{\gamma - 1}{\beta\gamma} \frac{\partial}{\partial t} p(z, t). \quad (\text{A.2})$$

Duhamel’s principle (see for example [22]) asserts that the solution to problem (A.1) is given by

$$\tau(r, z, t) = \int_0^t \tau_h(r, z, t - u, u) du, \quad (\text{A.3})$$

where τ_h is solution of the homogeneous problem given by:

$$\begin{cases} \left(\frac{\partial}{\partial t} - \alpha_t \nabla^2\right) \tau_h(r, z, t, u) = 0, \forall (r, z) \in \Omega, t > u, \\ \tau_h \text{ remains finite at } r = 0, \\ \tau_h(a, z, t, u) = 0, \quad \forall z \in [0, \ell], t > u, \\ \tau_h(r, 0, t, u) = 0 \text{ and } \tau_h(r, \ell, t, u) = 0, \forall r \in [0, a], t > u, \\ \tau_h(r, z, u, u) = \Phi(z, u), \quad \forall (r, z) \in \Omega, t = u, \end{cases} \quad (\text{A.4})$$

with $\Phi(z, u)$ as the initial source at time $t = u$. The homogeneous problem (A.4) is solved by using the method of separation of variables (see for example [22]) where τ_h takes the special form

$$\tau_h(r, z, t, u) = f(r)g(z)h(t). \quad (\text{A.5})$$

When taking into account the boundary conditions (A.4), the solutions for each of these functions can be obtained as follows:

$$h(t) = e^{-\sigma_t^2 \alpha_t t}, \quad (\text{A.6a})$$

$$f(r) = \sum_{n=1}^{+\infty} A_n J_0(\sigma_r r), \quad (\text{A.6b})$$

$$g(z) = \sum_{m=1}^{+\infty} B_m(u) \sin(\sigma_z z), \quad (\text{A.6c})$$

where $\sigma_r = j_n/a$, with j_n are the roots of $J_0(j_n) = 0$, $\sigma_z = m\pi/\ell$ and $\sigma_t^2 = \sigma_r^2 + \sigma_z^2$. The coefficients A_n and $B_m(u)$ are determined by the initial data of the auxiliary problem (A.4), namely:

$$A_n = \frac{\langle 1 | J_0(\sigma_r r) \rangle_S}{\langle J_0(\sigma_r r) | J_0(\sigma_r r) \rangle_S} = \frac{2}{j_n J_1(j_n)}, \quad (\text{A.7})$$

and

$$\begin{aligned} B_m(u) &= \frac{\langle \Phi(z, u) | \sin(\sigma_z z) \rangle_\ell}{\langle \sin(\sigma_z z) | \sin(\sigma_z z) \rangle_\ell} \\ &= \frac{2}{\ell} \int_0^\ell \Phi(z, u) \sin\left(\frac{m\pi}{\ell} z\right) dz. \end{aligned} \quad (\text{A.8})$$

Then, combining equations ((A.6a), (A.6b), (A.6c)) and (A.7), (A.8) with (A.9), the solution of the homogeneous problem (A.4) is given by

$$\begin{aligned} \tau_h(r, z, t, u) &= \sum_{m=1}^{+\infty} \sum_{n=1}^{+\infty} \frac{2}{j_n J_1(j_n)} J_0(j_n r/a) \\ &\quad \cdot \frac{2}{\ell} \sin\left(\frac{m\pi}{\ell} z\right) \int_0^\ell \Phi(z, u) \sin\left(\frac{m\pi}{\ell} z\right) dz \\ &\quad \cdot e^{-\alpha_t t \left[\left(\frac{m\pi}{\ell}\right)^2 + \left(\frac{j_n}{a}\right)^2 \right]}. \end{aligned} \quad (\text{A.9})$$

By Duhamel’s principle (A.3), evoking (A.9) and (A.2), the solution of the inhomogeneous problem (A.1) is given by

$$\begin{aligned} \tau(r, z, t) &= \frac{\gamma - 1}{\beta\gamma} \sum_{m=1}^{+\infty} \sum_{n=1}^{+\infty} \frac{4 J_0(j_n r/a)}{j_n \ell J_1(j_n)} \\ &\quad \cdot \sin\left(\frac{m\pi}{\ell} z\right) \int_0^\ell \sin\left(\frac{m\pi}{\ell} z\right) \\ &\quad \cdot \int_0^t \frac{\partial}{\partial t} p(z, u) e^{-\alpha_t(t-u) \left[\left(\frac{m\pi}{\ell}\right)^2 + \left(\frac{j_n}{a}\right)^2 \right]} du dz, \end{aligned} \quad (\text{A.10})$$

where the integral on du represents a convolution product which can be expressed by using the convolution theorem as a simple product in the Fourier domain. Thus, by using the basic properties of the Fourier transform, the integral part takes the form

$$\begin{aligned} &\int_0^t \frac{\partial}{\partial t} p(z, u) e^{-\alpha_t(t-u) \left[\left(\frac{m\pi}{\ell}\right)^2 + \left(\frac{j_n}{a}\right)^2 \right]} du \\ &= p(z, \omega) \frac{j\omega}{j\omega + \alpha_t \left[\left(\frac{m\pi}{\ell}\right)^2 + \left(\frac{j_n}{a}\right)^2 \right]}, \end{aligned} \quad (\text{A.11})$$

where $p(z, \omega) = \mathcal{F}(p(z, t))$ (\mathcal{F} being the Fourier transform operator).

Finally, the solution of $\tau(r, z)$ for a harmonic motion (the factor $e^{j\omega t}$ is omitted) is given by:

$$\tau(r, z) = \frac{\gamma - 1}{\beta\gamma} \sum_{m=1}^{+\infty} \sum_{n=1}^{+\infty} \frac{4J_0(j_n r/a)}{j_n \ell J_1(j_n)} \sin\left(\frac{m\pi}{\ell} z\right) \cdot \frac{1}{1 + \frac{\alpha_t}{j\omega} \left[\left(\frac{m\pi}{\ell}\right)^2 + \left(\frac{j_n}{a}\right)^2\right]} \int_0^\ell \sin\left(\frac{m\pi}{\ell} z\right) p(z) dz. \tag{A.12}$$

Appendix B. Solution of the propagation equation (21) by the LADM

The Laplace transform (denoted by \mathcal{L}_z) is applied on both sides of equation (21), namely

$$\mathcal{L}_z \left[\frac{\partial^2}{\partial z^2} p(z) \right] = -\chi_t^2 \mathcal{L}_z [p(z)] + \mathcal{L}_z \left[\alpha \sum_{m=1}^{+\infty} \sum_{n=1}^{+\infty} a_{m,n} \sin\left(\frac{m\pi}{\ell} z\right) \cdot \int_0^\ell \sin\left(\frac{m\pi}{\ell} z\right) p(z) dz \right]. \tag{B.1}$$

Using the basic properties of the Laplace transform and noting that the integral part of the equation is a constant, the previous equation takes the form

$$s^2 \mathcal{L}_z [p(z)] - sp(0) - p'(0) + \chi_t^2 \mathcal{L}_z [p(z)] = +\alpha \sum_{m=1}^{+\infty} \sum_{n=1}^{+\infty} a_{m,n} \mathcal{L}_z \left[\sin\left(\frac{m\pi}{\ell} z\right) \right] \cdot \int_0^\ell \sin\left(\frac{m\pi}{\ell} z\right) p(z) dz, \tag{B.2}$$

where $p(0)$ and $p'(0)$ are constants given by the boundary conditions (20a) and (20b). Then, rearranging the terms of the equation and invoking the Laplace transform of the sine function yields straightforwardly

$$\mathcal{L}_z [p(z)] = \frac{s}{s^2 + \chi_t^2} p(0) + \frac{1}{s^2 + \chi_t^2} p'(0) + \alpha \frac{1}{s^2 + \chi_t^2} \sum_{m=1}^{+\infty} \sum_{n=1}^{+\infty} a_{m,n} \frac{\left(\frac{m\pi}{\ell}\right)}{s^2 + \left(\frac{m\pi}{\ell}\right)^2} \cdot \int_0^\ell \sin\left(\frac{m\pi}{\ell} z\right) p(z) dz. \tag{B.3}$$

Hence, applying the inverse Laplace transform on both sides of equation (B.3), $p(z)$ is given by

$$p(z) = p(0) \cos(\chi_t z) + \frac{p'(0)}{\chi_t} \sin(\chi_t z) + \alpha \sum_{m=1}^{+\infty} \sum_{n=1}^{+\infty} a_{m,n} \phi_m(z) \cdot \int_0^\ell \sin\left(\frac{m\pi}{\ell} z\right) p(z) dz, \tag{B.4}$$

with

$$\phi_m(z) = \mathcal{L}_z^{-1} \left[\frac{1}{\chi_t} \frac{\chi_t}{s^2 + \chi_t^2} \frac{\left(\frac{m\pi}{\ell}\right)}{s^2 + \left(\frac{m\pi}{\ell}\right)^2} \right] = \frac{1}{\chi_t} \frac{\chi_t \sin\left(\frac{m\pi}{\ell} z\right) - \left(\frac{m\pi}{\ell}\right) \sin(\chi_t z)}{\chi_t^2 - \left(\frac{m\pi}{\ell}\right)^2}, \tag{B.5}$$

for $\chi_t \neq m\pi/\ell$. Since χ_t is a complex quantity, singularities $\chi_t = m\pi/\ell$ are not expected to occur. Therefore, to prevent unnecessary complexity in the formulation, the following equations exclude them.

The ADM [23] assumes that the solution of equation (B.4) can be represented in the form of an infinite series:

$$p(z) = \sum_{k=0}^{+\infty} p_k(z). \tag{B.6}$$

Then, replacing the general form of the solution (B.6) in (B.4), Adomian decomposition satisfies the following recurrence relation

$$p_0(z) = p(0) \cos(\chi_t z) + \frac{p'(0)}{\chi_t} \sin(\chi_t z), \tag{B.7}$$

for $k = 0$ and

$$p_k(z) = \alpha \sum_{m=1}^{+\infty} \sum_{n=1}^{+\infty} a_{m,n} \phi_m(z) \cdot \int_0^\ell \sin\left(\frac{m\pi}{\ell} z\right) p_{k-1}(z) dz, \tag{B.8}$$

for $k \geq 1$. Hence substituting equation (B.7) in (B.8), the term $p_1(z)$ is given by

$$p_1(z) = p(0) \alpha \sum_{m=1}^{+\infty} \sum_{n=1}^{+\infty} a_{m,n} \phi_m(z) \beta_{1,m} + \frac{p'(0)}{\chi_t} \alpha \sum_{m=1}^{+\infty} \sum_{n=1}^{+\infty} a_{m,n} \phi_m(z) \beta'_{1,m}, \tag{B.9}$$

with (noting that $\cos(m\pi) = (-1)^m$)

$$\beta_{1,m} = \int_0^\ell \sin\left(\frac{m\pi}{\ell} z\right) \cos(\chi_t z) dz = \frac{\frac{m\pi}{\ell} ((-1)^m \cos(\chi_t \ell) - 1)}{\chi_t^2 - \left(\frac{m\pi}{\ell}\right)^2}, \tag{B.10a}$$

$$\beta'_{1,m} = \int_0^\ell \sin\left(\frac{m\pi}{\ell} z\right) \sin(\chi_t z) dz = \frac{\frac{m\pi}{\ell} (-1)^m \sin(\chi_t \ell)}{\chi_t^2 - \left(\frac{m\pi}{\ell}\right)^2}. \tag{B.10b}$$

Combining the solution (B.9) for $p_1(z)$ with the recursive relation (B.8), the next term $p_2(z)$ is given by

$$p_2(z) = p(0) \alpha^2 \sum_{m=1}^{+\infty} \sum_{n=1}^{+\infty} a_{m,n} \phi_m(z) \beta_{2,m}$$

$$+ \frac{p'(0)}{\chi_t} \alpha^2 \sum_{m=1}^{+\infty} \sum_{n=1}^{+\infty} a_{m,n} \phi_m(z) \beta'_{2,m}, \tag{B.11}$$

with

$$\beta_{2,m} = \sum_{\nu=1}^{+\infty} \sum_{\mu=1}^{+\infty} a_{\nu,\mu} \beta_{1,\nu} \psi_{m,\nu}, \tag{B.12a}$$

$$\beta'_{2,m} = \sum_{\nu=1}^{+\infty} \sum_{\mu=1}^{+\infty} a_{\nu,\mu} \beta'_{1,\nu} \psi_{m,\nu}, \tag{B.12b}$$

and

$$\begin{aligned} \psi_{m,\nu} &= \int_0^\ell \sin\left(\frac{m\pi}{\ell} z\right) \phi_\nu(z) dz \\ &= \delta_{m,\nu} \frac{\ell/2}{\chi_t^2 - \left(\frac{m\pi}{\ell}\right)^2} \\ &\quad - \frac{\frac{1}{\chi_t} \frac{m\pi}{\ell} \frac{\nu\pi}{\ell} (-1)^m \sin(\chi_t \ell)}{\left(\chi_t^2 - \left(\frac{\nu\pi}{\ell}\right)^2\right) \left(\chi_t^2 - \left(\frac{m\pi}{\ell}\right)^2\right)}, \end{aligned} \tag{B.13}$$

with $\delta_{m,\nu}$ the Kronecker delta. Hence, the next terms $p_k(z)$ take the general form:

$$\begin{aligned} p_k(z) &= p(0) \alpha^k \sum_{m=1}^{+\infty} \sum_{n=1}^{+\infty} a_{m,n} \phi_m(z) \beta_{k,m} \\ &\quad + \frac{p'(0)}{\chi_t} \alpha^k \sum_{m=1}^{+\infty} \sum_{n=1}^{+\infty} a_{m,n} \phi_m(z) \beta'_{k,m}, \end{aligned} \tag{B.14}$$

where

$$\beta_{k,m} = \sum_{\nu=1}^{+\infty} \sum_{\mu=1}^{+\infty} a_{\nu,\mu} \beta_{k-1,\nu} \psi_{m,\nu}, \tag{B.15a}$$

$$\beta'_{k,m} = \sum_{\nu=1}^{+\infty} \sum_{\mu=1}^{+\infty} a_{\nu,\mu} \beta'_{k-1,\nu} \psi_{m,\nu}, \tag{B.15b}$$

are the recursive relations, the first terms being given by (B.10a) and (B.10b).

Appendix C. Determination of the constants $p(0)$, $p'(0)$ and $p(\ell)$

The boundary condition (20a) on diaphragm of the transmitter microphone at $z = 0$ provides directly the constant

$$p'(0) = \frac{\partial}{\partial z} p(0) = -Z_\nu S v_t. \tag{C.1}$$

The constant $p(0)$ is given by the second boundary condition (20b) on diaphragm of the receiver microphone at $z = \ell$

$$\frac{\partial}{\partial z} p(\ell) = -Z_\nu Y_r p(\ell). \tag{C.2}$$

Evoking equations (B.6), (B.7) and (B.14) and their derivatives with respect to the coordinate z , produces the relation

$$\begin{aligned} &-p(0) \chi_t \sin(\chi_t \ell) + p'(0) \cos(\chi_t \ell) \\ &+ p(0) \sum_{k=1}^{+\infty} \alpha^k \sum_{m=1}^{+\infty} \sum_{n=1}^{+\infty} a_{m,n} \phi'_m(\ell) \beta_{k,m} \\ &+ \frac{p'(0)}{\chi_t} \sum_{k=1}^{+\infty} \alpha^k \sum_{m=1}^{+\infty} \sum_{n=1}^{+\infty} a_{m,n} \phi'_m(\ell) \beta'_{k,m} \\ &= -Z_\nu Y_r p(0) \cos(\chi_t \ell) - Z_\nu Y_r \frac{p'(0)}{\chi_t} \sin(\chi_t \ell) \\ &\quad - Z_\nu Y_r p(0) \sum_{k=1}^{+\infty} \alpha^k \sum_{m=1}^{+\infty} \sum_{n=1}^{+\infty} a_{m,n} \phi_m(\ell) \beta_{k,m} \\ &\quad - Z_\nu Y_r \frac{p'(0)}{\chi_t} \sum_{k=1}^{+\infty} \alpha^k \sum_{m=1}^{+\infty} \sum_{n=1}^{+\infty} a_{m,n} \phi_m(\ell) \beta'_{k,m}, \end{aligned} \tag{C.3}$$

with

$$\phi'_m(z) = \frac{\frac{m\pi}{\ell} \cos\left(\frac{m\pi}{\ell} z\right) - \left(\frac{m\pi}{\ell}\right) \cos(\chi_t z)}{\chi_t^2 - \left(\frac{m\pi}{\ell}\right)^2}. \tag{C.4}$$

Rearranging the terms in equations (C.3) and using (C.1) yields straightforwardly

$$p(0) = \frac{Z_\nu S v_t C_0 + Z_\nu Y_r D_0}{\chi_t A_0 + Z_\nu Y_r B_0}, \tag{C.5}$$

with

$$A_0 = -\chi_t \sin(\chi_t \ell) + \sum_{k=1}^{+\infty} \alpha^k \sum_{m=1}^{+\infty} \sum_{n=1}^{+\infty} a_{m,n} \phi'_m(\ell) \beta_{k,m}, \tag{C.6a}$$

$$B_0 = \cos(\chi_t \ell) + \sum_{k=1}^{+\infty} \alpha^k \sum_{m=1}^{+\infty} \sum_{n=1}^{+\infty} a_{m,n} \phi_m(\ell) \beta_{k,m}, \tag{C.6b}$$

$$C_0 = \chi_t \cos(\chi_t \ell) + \sum_{k=1}^{+\infty} \alpha^k \sum_{m=1}^{+\infty} \sum_{n=1}^{+\infty} a_{m,n} \phi'_m(\ell) \beta'_{k,m}, \tag{C.6c}$$

$$D_0 = \sin(\chi_t \ell) + \sum_{k=1}^{+\infty} \alpha^k \sum_{m=1}^{+\infty} \sum_{n=1}^{+\infty} a_{m,n} \phi_m(\ell) \beta'_{k,m}. \tag{C.6d}$$

Finally, invoking expressions (B.6), (B.7), (B.14) and (C.6b), (C.6d), the pressure $p(\ell)$ is given by

$$p(\ell) = p(0) B_0 + \frac{p'(0)}{\chi_t} D_0. \tag{C.7}$$

ORCID iD

D Rodrigues  <https://orcid.org/0000-0002-4695-9466>

References

- [1] IEC 61094-2:2009 2009 Measurement microphones-part2: primary method for the pressure calibration of laboratory standard microphones by the reciprocity method IEC standard
- [2] Rodrigues D *et al* 2023 Final report on the key comparison CCAUV.A-K6 Metrologia 60 09001

- [3] Daniels F 1947 Acoustical impedance of enclosures *J. Acoust. Soc. Am.* **19** 569–71
- [4] Biagi F and Cook R 1954 Acoustic impedance of a right circular cylindrical enclosure *J. Acoust. Soc. Am.* **26** 506–9
- [5] Gerber H 1964 Acoustic properties of fluid-filled chambers at infrasonic frequencies in the absence of convection *J. Acoust. Soc. Am.* **36** 1427–34
- [6] Riéty P and Lecollinet M 1974 Le dispositif d'étalonnage primaire des microphones de laboratoire de l'institut national de métrologie *Metrologia* **10** 17
- [7] Ballagh K O 1987 Acoustical admittance of cylindrical cavities *J. Sound Vib.* **112** 567–9
- [8] Jarvis D R 1987 Acoustical admittance of cylindrical cavities *J. Sound Vib.* **117** 390–2
- [9] Rasmussen K 2004 Datafiles simulating a pressure reciprocity calibration of microphones *EUROMET Project 294—Reort PL-13a*
- [10] Guianvarc'h C, Durocher J-N, Bruneau M and Bruneau A-M 2006 Acoustic transfer admittance of cylindrical cavities *J. Sound Vib.* **292** 595–603
- [11] Olsen E and Frederiksen E 2013 Microphone acoustic impedance in reciprocity calibration of laboratory standard microphone *INTER-NOISE and NOISE-CON Congress and Conf. Proc.* vol 247 pp 679–86
- [12] Jackett R 2014 The effect of heat conduction on the realization of the primary standard for sound pressure *Metrologia* **51** 423
- [13] Vincent P, Rodrigues D, Larsonnier F, Guianvarc'h C and Durand S 2018 Acoustic transfer admittance of cylindrical cavities in infrasonic frequency range *Metrologia* **56** 015003
- [14] Erling Sandermann O 2020 Next steps in development of transfer impedance calculation of couplers for reciprocity calibration of laboratory standard microphones *Forum Acusticum (Lyon, France)* pp 2233–9
- [15] Rodrigues D, Vincent P, Barham R, Larsonnier F and Durand S 2022 A laser pistonphone designed for absolute calibration of infrasound sensors from 10 mHz up to 20 Hz *Metrologia* **60** 015004
- [16] BIPM 2022 Strategy 2021 to 2031, Consultative Committee for Acoustics, Ultrasound, and Vibration (CCAUV) *BIPM Report* (available at: www.bipm.org/fr/committees/cc/ccauv)
- [17] IEC 61094-2:2009/AMD1:2022 2022 Amendment 1—electroacoustics—measurement microphones—part 2: primary method for pressure calibration of laboratory standard microphones by the reciprocity technique *IEC standard*
- [18] Rasmussen K 1993 Radial motion-wave in cylindrical plane-wave couplers *Acta Acust.* **1** 145–51
- [19] Bruneau M and Scelo T 2006 *Fundamentals of Acoustics* (ISTE)
- [20] Lavergne T, Joly N and Durand S 2013 Acoustic thermal boundary condition on thin bodies: application to membranes and fibres *Acta Acust. Acust.* **99** 524–36
- [21] Guianvarc'h C, Durocher J-N, Bruneau M and Bruneau A-M 2006 Improved formulation of the acoustic transfer admittance of cylindrical cavities *Acta Acust. Acust.* **92** 345–54
- [22] Lawrence C E 2010 *Partial Differential Equations* (American Mathematical Society)
- [23] Adomian G 1988 A review of the decomposition method in applied mathematics *J. Math. Anal. Appl.* **135** 501–44
- [24] Kwong Mak M, Sing Leung C and Harko T 2021 A brief introduction to the Adomian decomposition method, with applications in astronomy and astrophysics *Rom. Astron. J.* **31** 201–40
- [25] Steer M B and Edwards T C 2000 *Foundations of Interconnect and Microstrip Design (Appendix A: Transmission Line Theory)* (Wiley) pp 435–47
- [26] IEC TR 61094-10: 2022 2022 Electroacoustics—measurement microphones—part 10: Absolute pressure calibration of microphones at low frequencies using calculable pistonphones *IEC Standard*